

The predictive significance of chromobox family members in prostate cancer in humans

Xiaoting Xu

Department of Urology, Sun Yat-sen Memorial Hospital, Sun Yat-sen University

Cong Lai

Department of Urology, Sun Yat-sen Memorial Hospital, Sun Yat-sen University

Jiawen Luo

Department of Urology, Sun Yat-sen Memorial Hospital, Sun Yat-sen University

Juanyi Shi

Department of Urology, Sun Yat-sen Memorial Hospital, Sun Yat-sen University

Kaixuan Guo

Department of Urology, Sun Yat-sen Memorial Hospital, Sun Yat-sen University

Jintao Hu

Department of Urology, Sun Yat-sen Memorial Hospital, Sun Yat-sen University

Yelisudan Mulati

Department of Urology, Sun Yat-sen Memorial Hospital, Sun Yat-sen University

Yunfei Xiao

Department of Urology, Sun Yat-sen Memorial Hospital, Sun Yat-sen University

Degeng Kong

Department of Urology, Sun Yat-sen Memorial Hospital, Sun Yat-sen University

Cheng Liu

Department of Urology, Sun Yat-sen Memorial Hospital, Sun Yat-sen University

Jingang Huang

Medical Research Center, Guangdong Provincial Key Laboratory of Malignant Tumor Epigenetics and Gene Regulation, Guangdong-Hong Kong Joint Laboratory for RNA Medicine, Sun Yat-Sen Memorial Hospital

Kewei Xu

xukewei@mail.sysu.edu.cn

Department of Urology, Sun Yat-sen Memorial Hospital, Sun Yat-sen University

Research Article

Keywords: Prostate cancer, Chromobox, Enrichment analysis, Nomogram, Prognosis

Posted Date: September 6th, 2023

DOI: <https://doi.org/10.21203/rs.3.rs-3294410/v1>

License: © ⓘ This work is licensed under a Creative Commons Attribution 4.0 International License.

[Read Full License](#)

Additional Declarations: No competing interests reported.

Version of Record: A version of this preprint was published at Cellular Oncology on March 1st, 2024. See the published version at <https://doi.org/10.1007/s13402-024-00929-7>.

Abstract

Purpose The Chromobox (CBX) family proteins are crucial elements of the epigenetic regulatory machinery and play a significant role in the development and advancement of cancer. Nevertheless, there is limited understanding regarding the role of CBXs in development or progression of prostate cancer (PCa). Our objective is to develop a unique prognostic model associated with CBXs to improve the accuracy of predicting outcomes of patients with PCa.

Methods Transcriptome sequencing and clinical data for PCa were obtained from the Cancer Genome Atlas and Gene Expression Omnibus databases. The data was then analyzed to identify differential expression, assess prognostic value, determine gene pathway enrichment, and evaluate immune cell infiltration. COX regression analysis was utilized to identify the independent prognostic factors that impact disease-free survival (DFS) in PCa, and subsequently, a nomogram was created. In vitro proliferation, migration and invasion assay were conducted to examine the function of CBX2 in PCa.

Results CBX2, CBX3, CBX4, and CBX8 were upregulated, whereas CBX6 and CBX7 were downregulated in PCa tumor tissues. The expression level of these genes differs depending on the cancer's stage and grade. A negative outcome is associated with patients who have elevated levels of CBX1, CBX2, CBX3, CBX4 and CBX8 expression. An independent prognostic factors for PCa were the expression level of CBX2 and T stage, as well as Gleason score, as determined by Cox regression analysis. Additionally, a nomogram was created. The infiltration level of various immune cells is associated with the expression level of CBX2. In vitro studies have shown that the knockdown of CBX2 can greatly impede the growth, migration and invasion of PCa cells.

Conclusion CBX2 is involved in the development and advancement of PCa, suggesting its potential as a reliable prognostic indicator for PCa patients.

1 Introduction

Prostate cancer (PCa) ranks as the fifth most prevalent malignant neoplasm worldwide and the second most frequent among males, contributing significantly to cancer-related mortalities in men. Based on pertinent data, the year 2020 witnessed a total of 1,414,259 fresh instances of PCa worldwide, resulting in 375,304 fatalities [1]. The outlook for initial, confined PCa is generally positive, whereas advanced PCa carries a bleak prognosis, often leading to metastasis following chemotherapy, surgery, and radiotherapy. The survival rate after 5 years is merely 32%[2]. The prognosis is significantly influenced by the recurrence of PCa at a biochemical level, as it escalates the chances of clinical metastasis, advancement, and fatality caused by PCa[3, 4]. Nevertheless, the limited understanding of the molecular mechanisms implicated in the progression of PCa severely impedes clinicians' ability to formulate accurate treatment approaches for patients experiencing biochemical recurrence. Therefore, constructing accurate prognostic models for PCa is especially crucial.

Accumulating evidence suggests that epigenetics plays a significant role in the growth and advancement of PCa through diverse mechanisms, including DNA methylation, interaction between DNA methylation and histone modification, and control of non-coding RNAs[5]. CBX proteins, belonging to the CBX family, play a crucial role in epigenetic modification processes as significant regulatory factors within polycomb (Pc) repressive complex 1 (PRC1). So far, the human genome has revealed the presence of eight CBX proteins that exhibit comparable chemical compositions. These proteins possess a solitary N-terminal chromodomain and are denoted by the Chromobox they encode at their N-terminus. HP1 proteins, including CBX1, CBX3, and CBX5, are crucial elements of heterochromatin-mediated gene silencing due to the distinct structures of the C-terminus of CBX proteins. (2) CBX2, CBX4, CBX6, CBX7, and CBX8, which are alternatively referred to as Pc proteins. Pc proteins contain common structural domains such as the N-terminal chromodomain, the C-terminal PcRbox, and the DNA-binding region adjacent to the N-terminus, with different structural domains in between. Each CBX protein has epigenetic regulatory functions and represses target gene transcription through chromatin modification[6, 7]. Numerous studies have indicated that CBX family proteins contribute to the onset and advancement of various malignancies, such as colorectal cancer[8], lung adenocarcinoma[9], ovarian cancer[10], esophageal cancer[11], and several others[12]. However, the precise involvement of CBXs in the progression of prostate cancer remains uncertain.

This study examined various aspects including differential expression, prognostic significance, gene pathway enrichment, and immune cell infiltration by utilizing publicly available databases. Additionally, a prognostic model was developed to predict DFS in individuals diagnosed with PCa. Moreover, the in vitro experiments confirmed the molecular mechanisms through which the signature molecules control the behavior of PCa.

2 Materials and Methods

2.1 Collection and preprocessing of PCa data

Data from the TCGA database (<https://portal.gdc.cancer.gov>) and the GEO database (<https://www.ncbi.nlm.nih.gov/geo/,GSE70770>) were obtained, including transcriptome sequencing data and clinical data for PCa tissue and adjacent tissue. Patients who had missing information were excluded from the study, and the acquired data was systematically organized and standardized in preparation for subsequent analysis. Immunohistochemical staining images of CBXs in PCa tumor tissue and adjacent tissue were obtained from The Human Protein Atlas (THPA) database (<https://www.proteinatlas.org/>). CBXs (CBX1, CBX2, CBX3, CBX4, CBX5, CBX6, CBX7, CBX8) were retrieved from the National Library of Medicine (<https://www.ncbi.nlm.nih.gov/gene/>).

2.2 Clinical relevance analysis of CBXs in PCa

The expression matrix of CBXs in PCa tumor tissue and adjacent tissue was obtained. To compare the levels of CBXs expression in paired PCa tumor and adjacent tissue, paired comparison plots were generated by GraphPad Prism. Utilizing clinical data from the TCGA database, including TNM staging

and Gleason scores, bar graphs were utilized to compare the variations in CBXs expression levels among PCa patients with various Gleason scores and TNM stages.

2.3 Prognostic analysis of CBXs in PCa

We obtained additional information and the CBXs expression matrix for patients with PCa from the TCGA and GEO databases. The patients were categorized into low-expression and high-expression groups of CBXs using the median expression level of CBXs as the threshold value. To assess if there was a variation in progression-free survival (PFS) among patients in the high- and low-expression groups of CBXs, Kaplan-Meier survival curves were generated by GraphPad Prism (version 8.0.1) and the findings were confirmed through the GEO database (GSE70770).

2.4 Construction of nomogram and prediction of DFS

To assess if the expression levels of CBXs and clinical characteristics were independent prognostic factors for patients, univariate and multivariate Cox analyses were conducted using patients' age, TNM stage, Gleason score, and other clinical data. The multivariate Cox regression analysis results were used to construct a nomogram. The prognosis of patients was evaluated using the 2-year, 3-year, and 5-year DFS, while the accuracy of the nomogram was indicated by the area under the receiver operating characteristic (ROC) curve (AUC). Validation of the prognostic model's predictive performance was subsequently conducted through the utilization of calibration curves and decision curve analysis (DCA). The accuracy of the findings was confirmed by utilizing GEO validation dataset (GSE70770).

2.5 Correlation between CBXs and immune status in PCa

Using immune cell-associated gene sets, the infiltration levels of immune cells in PCa tissue were analyzed through single-sample gene set enrichment analysis (ssGSEA). Pearson correlation analysis was utilized to calculate the association between levels of immune cell infiltration and expression of CBXs. Dot plots were utilized to compare the disparities in immune cell infiltration between the high- and low-expression groups of CBXs.

2.6 Analysis of enrichment using GSEA

To obtain differentially expressed genes between the high- and low-expression groups of CBXs, an analysis of differential expression was conducted. To identify the activated signaling pathways when CBXs were highly or lowly expressed, GSEA enrichment analysis (GSEA 4.2.3) was conducted using the differentially expressed genes.

2.7 Cultured cell lines

Human PCa cell lines PC3 and DU145 were obtained from the American Type Culture Collection (ATCC, VA, USA). PC3 and DU145 were grown in RPMI-1640 (Gibco, NY, USA) and DMEM (Gibco, NY, USA) medium respectively. In both medium, 10% fetal bovine serum (FBS, BI, Israel), 100 U/ml penicillin, and 100 mg/ml streptomycin have been added. The cells were grown in a temperature-controlled incubator containing 5% carbon dioxide at a temperature of 37 degrees Celsius.

2.8 RNA Interference

IBSBIO (Shanghai, China) synthesized and purified siRNA duplexes that specifically targeted the human CBX2 gene. Human PCa cells (1×10^5) were seeded in six-well plates and grown until they reached 50%-70% confluence. At this stage, Lipofectamine iMAX (Invitrogen, USA) was used for transient transfection following the guidelines provided by the manufacturer. Supplementary file (Table S1-S2) contains the confirmed oligo sequences for siRNA and primer pairs for qPCR.

2.9 CCK8 assay

Cell growth was detected using the Cell Counting Kit-8 (APEX BIO, USA) following the guidelines provided by the manufacturer. Cells were seeded and cultured at a density of 1×10^3 /well in 100 μ L of medium into 96-well microplates (Corning, USA). 10 μ L of CCK-8 reagent was added to corresponding well every 24 hours in 5 days. The absorbance which represents the cell count was analyzed at 450 nm using microplate reader (TECAN Spark, Switz) after 2 hours of incubation, and the cell proliferation curve was drawn by GraphPad Prism (version 8.0.1).

2.10 Transwell Assay

After 48 hours of temporary transfection with siRNA, the cells were collected and underwent invasion or migration tests using chambers (8 μ m, Corning, USA) with or without Matrigel (BD Science, USA). Around 50,000 cells were suspended in 200 milliliters of medium without serum and placed in the upper chambers, while the lower chambers were filled with 600 microliters of medium containing 10% FBS. Following a 24-hour incubation period, the remaining cells in the upper chamber were eliminated using cotton swabs. Subsequently, cells on the lower surface were fixed using paraformaldehyde and stained with 0.1% crystal violet for 20 minutes at ambient temperature. Photographs were taken using a 400x magnification microscope (Olympus, Tokyo, Japan) in five randomly selected areas. The ImageJ software was used to count the cells.

2.11 Western blot

Protein samples were prepared and separated by SDS-PAGE gels, blotted onto PVDF membrane, and blocked with 5% non-fat milk. Then, blots were hybridized with the following primary antibodies: CBX2 (#31050, Signalway Antibody, USA), GAPDH (GB11002, Servicebio, China).

2.12 Statistical analysis

R software (R 4.2.2) and GraphPad Prism (version 8.0.1) were used for all statistical analyses. Pearson correlation analysis determined the correlation. Statistical analysis involved the use of chi-square tests and *t*-tests to compare clinical variables and measured values across two groups. Cox regression analysis was used to evaluate the survival status. Survival curves were produced using the Kaplan-Meier technique and assessed using the log-rank test. Statistical significance was indicated by a two-tailed *p*-value less than 0.05.

3 Results

3.1 The clinical relevance of CBXs

In PCa tumor tissues, CBX2, CBX3, CBX4, and CBX8 exhibited elevated expression levels compared to adjacent non-tumor tissues according to paired comparison charts (Fig. 1b-d, h. $P < 0.001$). Conversely, CBX6 and CBX7 were demonstrated to be decreased (Fig. 1f, g. $P < 0.001$). No difference was observed between CBX1 and CBX5 (Fig. 1a, e). Images of CBXs stained with immunohistochemical methods were acquired from the THPA database (Fig. 2a-h). In T3 and T4 PCa tissues, the violin charts indicated increased expression levels of CBX1, CBX2, CBX3, and CBX8 compared to T2 (Fig. 3a-c, h. $P < 0.05$). Additionally, CBX1 exhibited higher expression in T4 than in T3 (Fig. 3a). There were no variations observed in CBX4, CBX5, CBX6, and CBX7 among different T stages (Fig. 3d-g). In N1 PCa tissues, the violin charts indicated elevated expression levels of CBX1, CBX2, CBX3, CBX4, and CBX8 compared to N0 (Fig. 4a-d, h. $P < 0.001$). However, there were no significant differences observed for CBX5, CBX6, and CBX7 between different N stages (Fig. 4e-g). The violin plots indicated that the M1 PCa tissues exhibited elevated expression levels of CBX1 and CBX2 compared to M0 (Fig. 5a, b. $P < 0.05$), whereas CBX7 expression was higher in M0 than M1 (Fig. 5g). There was no variation observed in CBX3, CBX4, CBX5, CBX6, and CBX8 among various M stages (Fig. 5c-f, h). In Gleason ≥ 8 group PCa tissues, the violin charts indicated elevated expression levels of CBX1, CBX2, CBX3, CBX4, and CBX8 compared to the Gleason ≤ 7 group (Fig. 6a-d, h. $P < 0.001$). Conversely, the Gleason ≤ 7 group exhibited higher expression of CBX7 compared to the Gleason ≥ 8 group (Fig. 6g). The expression of CBX5 and CBX6 was similar in PCa tissues with different Gleason scores (Fig. 6e, f).

3.2 Prognostic analysis of CBXs

The TCGA database was used to generate survival curves, which compared DFS between two groups: high expression and low expression of CBXs. The results indicated that patients with high expression levels of CBX1, CBX2, CBX3, CBX4, and CBX8 had a poorer prognosis (Fig. 7a-d, h. $P < 0.05$). Prognosis did not vary between the high and low expression groups of CBX5, CBX6, and CBX7 (Fig. 7e-g)

3.3 Construction of nomogram and prediction of DFS

The independent prognostic factors for patients, as shown in Table S3, were the expression of CBX2 and T, as well as the Gleason score, according to the results of both univariate and multivariate Cox analysis. Based on the findings of the multivariate Cox regression analysis (Fig. 8a), a nomogram was constructed. The model demonstrated high accuracy based on the calibration curves (Fig. 8b-d). ROC curves showed that the AUC for 2-year, 3-year, and 5-year DFS were 0.708, 0.734, and 0.738, respectively, as shown in Fig. 8e-g. The prognostic model demonstrated excellent predictive performance according to the DCA curves (Fig. 8h-j). The validation of the aforementioned findings was conducted using the dataset GSE70770. The model demonstrated exceptional accuracy in the calibration curves of the validation set (Fig. 9a-c). In Fig. 9d-f, the ROC curves of the validation set indicated that the AUC for 2-year, 3-year, and

5-year DFS were 0.693, 0.700, and 0.723, correspondingly. The prognostic model demonstrated good predictive performance in the validation set, as indicated by the DCA curves (Fig. 9g-i).

3.4 Infiltration of immune cells in PCa patients with CBX2

A lollipop plot was created using the ssGSEA analysis results to illustrate the relationship between CBX2 and genes related to the immune system (Fig. 10a). The dot plots indicated that the levels of Th2 cells, activated-DC, Macrophages, and Treg cells infiltrating the CBX2 high expression group were greater compared to the CBX2 low expression group (Fig. 10b-e, $P < 0.05$). The levels of infiltration by Th17 cells, Mast cells, and NK cells were higher in the group with low expression of CBX2 compared to the group with high expression of CBX2 (Fig. 10f-h, $P < 0.001$). These results suggest that increased CBX2 levels could be associated with the immunosuppressive tumor environment of PCa, while decreased levels could enhance the host's anti-tumor immunity.

3.5 GSEA enrichment analysis

The results of GSEA enrichment analysis indicated that the p53 signaling pathway, mismatch repair, cell cycle, TGF-beta signaling pathway, DNA replication, and homologous recombination are among the activated signaling pathways when CBX2 is expressed at high levels (Fig. 11a-f, $P < 0.05$). These findings suggest that CBX2 may have multifaceted functions in PCa. It can affect cell apoptosis, proliferation, and DNA damage response, contributing to tumor development and advancement. Additionally, CBX2 regulates the mismatch repair pathway, influencing DNA stability and mutation rate, which plays a role in tumor evolution and resistance to drugs. Moreover, it controls the cell cycle pathway, affecting cell division and arrest, thereby contributing to tumor growth and invasion. Furthermore, CBX2 regulates the TGF-beta signaling pathway, influencing cell differentiation, migration, angiogenesis, and immune suppression, thereby contributing to tumor metastasis and evasion of the immune system. Lastly, it may also have a significant impact on the cell cycle, maintaining chromosome stability, responding to DNA damage, and promoting genetic variation.

3.6 The effect of CBX2 on the proliferation, migration and invasion of PCa Cells

The function of CBX2 in PCa has been investigated in several studies, but its role remains incompletely understood. In order to clarify the function of CBX2 in the growth of PCa cells, CBX2 was first knocked down in PC3 and DU145 cell lines as evidenced by qPCR (Fig. 12a) and WB (Fig. 12b). The CCK-8 assay conducted afterwards which demonstrated that the proliferation of PCa cells was inhibited by the knockdown of CBX2 (Fig. 12c, d), suggesting that CBX2 plays a role in promoting PCa cell proliferation. Based on these results, we assessed the migratory and invasive capacities of PC3 and DU145 cells after suppressing CBX2. The findings showed that the suppression of CBX2 greatly reduced the ability of PCa cells to invade and migrate (Fig. 12e-g). The results confirmed that CBX2 has a vital role in regulating the advancement of PCa.

Discussion

PCa has a complex pathogenesis and is characterized as a disease that progresses through multiple stages. Although there has been significant advancement in the identification and management of PCa over the last few decades, the occurrence of early relapse following treatment remains a significant obstacle. Several research studies have indicated that, apart from tumor genetics, the abnormal regulation of epigenetics also has a crucial impact on the progression of PCa. Although the exact roles of CBXs in PCa are still not completely understood, previous studies have indicated that CBXs, which are essential constituents of epigenetic regulatory complexes, play significant roles in the advancement and growth of different types of cancer[16-21]. This study involved a comprehensive examination of their expression patterns and explored their associations with clinical features, prognostic importance, infiltration of immune cells, and potential functions in PCa. By employing bioinformatics, we have created a prognostic model that incorporates CBX2 and demonstrates exceptional predictive precision.

The findings of our study indicated that CBX2, CBX3, CBX4, and CBX8 exhibit increased expression in PCa tumor tissues, whereas CBX6 and CBX7 display decreased expression. Likewise, in cases of Diffuse large B-cell lymphoma (DLBCL), the levels of CBX2 mRNA and protein were elevated in DLBCL tissues compared to the control groups[16]. CBX2 expression levels were significantly elevated in cervical cancer tissues[18]. Elevated CBX2 levels have also been detected in cases of breast and bladder malignancies[19-22]. Downregulation of CBX6/7 has been confirmed in studies of multiple tumor types[23].

An additional unique discovery is that individuals with elevated levels of CBX1, CBX2, CBX3, CBX4, and CBX8 exhibited an unfavorable outlook, wherein the presence of CBX2 expression acted as a separate predictive factor for prognosis. Likewise, in research on ovarian cancer, CBX2 was among six genes employed to create a diagnostic and prognostic framework relying on the gene model associated with differentially expressed stem cells. This model serves as a powerful diagnostic biomarker and can define clinicopathological characteristics[24]. Another research study discovered that the expression of CBX1-3 mRNA might be indicative of unfavorable outcomes in terms of overall survival (OS) and PFS in individuals diagnosed with ovarian cancer[25]. Research on hepatocellular carcinoma established a new 4-gene signature (CDCA8, CBX2, UCK2, and SOCS2) that demonstrated excellent prognostic independence[26]. In a separate investigation on breast cancer, increased CBX2 expression was found to be strongly linked to worse OS and PFS in patients with breast cancer[27].

Regarding tumor immunity, we observed a correlation between the expression level of CBX2 and the degree of infiltration by various immune cells. Increased CBX2 expression could potentially be linked to the immunosuppressive microenvironment of PCa, whereas decreased expression might bolster the host's immune response to combat the tumor. In a study on gastric cancer, a comparable outcome was observed, where the levels of CBX2 and CBX8 expression hindered the infiltration of CD8+ T cells, macrophages, neutrophils, and dendritic cells[28]. Regarding other members of CBX, CBX6 might hinder M1 polarization and encourage Treg recruitment in the tumor microenvironment, potentially leading to an unfavorable prognosis in patients. Conversely, CBX7 could enhance the prognosis in patients with

bladder cancer by elevating the population of resting mast cells and reducing the content of macrophage M0.

Due to the significant role that CBX2 plays in different types of cancers, there are ongoing efforts to utilize CBX2 as a potential target for therapy. Brubaker et al. conducted a study where they created a peptide that blocks CBX2. They found that this peptide effectively suppressed the growth of ovarian cancer cells in both 2D and 3D environments. Additionally, it reduced the expression of a gene targeted by CBX2 and hindered tumor growth in vivo[29]. Di Costanzo et al. conducted an in vitro study confirming that vorinostat, an HDAC inhibitor, enhances the stability of CBX2 through SUMO-triggered ubiquitin-mediated pathways, thereby exerting its anti-leukemic effect[30].

This work has some limitations. The majority of the data used for analysis primarily came from online platforms. To fully validate the findings of this study, it is crucial to conduct additional experiments both in laboratory settings and living organisms, along with clinical trials. Moreover, the investigation into the roles and governing mechanisms of CBXs is excessively basic. Additional investigations are necessary to elucidate the precise correlation between every CBXs constituent and PCa.

To summarize, we initially conducted a comprehensive investigation into the manifestation of CBXs, its association with clinical characteristics, prognostic significance, infiltration of immune cells, and potential roles in PCa. With remarkable predictive accuracy, we developed a prognostic model that integrates CBX2. Experiments conducted in vitro have substantiated the crucial involvement of CBX2 in the proliferation, migration, and invasion of PCa cells. By establishing a theoretical foundation, this enables the development of clinical decision-making strategies that rely on prognosis and the discovery of novel tumor biomarkers and therapeutic targets.

Declarations

Ethical Approval

Not applicable.

Competing interests

The authors have no competing interests to declare that are relevant to the content of this article.

Authors' contributions

K.W.X. and J.G.H. designed and directed the research. X.T.X. and C.L. analyzed the data and drafted the manuscript. J.W.L. performed the in vitro experiments and revised the manuscript. J.Y.S., K.X.G. and J.T.H. collected references and revised the manuscript. Y.M., Y.F.X. and D.G.K. were responsible for cell culture and data collection. C.L. revised the manuscript. The final manuscript was approved by all authors.

Funding

Guangdong Province key areas research and development plan (2023B1111030006), National Natural Science Foundation of China (82072841 and 82372766), Natural Science Foundation of Guangdong Province (2021A1515010199), Key Areas Research and Development Program of Guangdong (2020B111114002), Guangdong Provincial Clinical Research Center for Urological Diseases (2020B1111170006) and Guangdong Science and Technology Department (2020B1212060018). Fundamental Research Funds for the Central Universities, Sun Yat-sen University (1320223001)

Availability of data and materials

The data for bioinformatics analysis are publicly accessible, and the specific details can be found in the materials and methods section of the paper.

References

1. H. Sung, J. Ferlay, R.L. Siegel, M. Laversanne, I. Soerjomataram, A. Jemal, F. Bray, *CA Cancer J Clin.* **71**, 209–249 (2021). 10.3322/caac.21660
2. R.L. Siegel, K.D. Miller, H.E. Fuchs, A. Jemal, *CA Cancer J Clin.* **72**, 7–33 (2022). 10.3322/caac.21708
3. S. Gillessen, A. Bossi, I.D. Davis, J. de Bono, K. Fizazi, N.D. James, N. Mottet, N. Shore, E. Small, M. Smith, C. Sweeney, B. Tombal, E.S. Antonarakis, A.M. Aparicio, A.J. Armstrong, G. Attard, T.M. Beer, H. Beltran, A. Bjartell, P. Blanchard, A. Briganti, R.G. Bristow, M. Bulbul, O. Caffo, D. Castellano, E. Castro, H.H. Cheng, K.N. Chi, S. Chowdhury, C.S. Clarke, N. Clarke, G. Daugaard, M. De Santis, I. Duran, R. Eeles, E. Efstathiou, J. Efstathiou, O. Ngozi Ekeke, C.P. Evans, S. Fanti, F.Y. Feng, V. Fonteyne, N. Fossati, M. Frydenberg, D. George, M. Gleave, G. Gravis, S. Halabi, D. Heinrich, K. Herrmann, C. Higano, M.S. Hofman, L.G. Horvath, M. Hussain, B.A. Jereczek-Fossa, R. Jones, R. Kanesvaran, P.L. Kellokumpu-Lehtinen, R.B. Khamli, L. Klotz, G. Kramer, R. Leibowitz, C.J. Logothetis, B.A. Mahal, F. Maluf, J. Mateo, D. Matheson, N. Mehra, A. Merseburger, A.K. Morgans, M.J. Morris, H. Mrabti, D. Mukherji, D.G. Murphy, V. Murthy, P.L. Nguyen, W.K. Oh, P. Ost, J.M. O'Sullivan, A.R. Padhani, C. Pezaro, D.M.C. Poon, C.C. Pritchard, D.M. Rabah, D. Rathkopf, R.E. Reiter, M.A. Rubin, C.J. Ryan, F. Saad, J. Pablo, O.A. Sade, H.I. Sartor, N. Scher, I. Sharifi, H. Skoneczna, D.E. Soule, S. Spratt, C.N. Srinivas, T. Sternberg, H. Steuber, M.R. Suzuki, M.E. Sydes, D. Taplin, L. Tilki, F. Turkeri, H. Turco, H. Uemura, Y. Uemura, C.L. Urun, I. van Vale, *Eur. Urol.* **83**, 267–293 (2023). Oort, N. Vapiwala, J. Walz, K. Yamoah, D. Ye, E.Y. Yu, A. Zapatero, T. Zilli and A. Omlin. 10.1016/j.eururo.2022.11.002
4. N.I. Simon, C. Parker, T.A. Hope, C.J. Paller, *Am. Soc. Clin. Oncol. Educ. Book.* **42**, 1–8 (2022). 10.1200/EDBK_351033
5. S. Goel, V. Bhatia, T. Biswas, B. Ateeq, *Semin Cancer Biol.* **83**, 136–151 (2022). 10.1016/j.semcancer.2021.01.009
6. J. Kim, R.E. Kingston, *J. Biosci.* **45**, (2020)

7. R.G. Ma, Y. Zhang, T.T. Sun, B. Cheng, J. Zhejiang Univ. Sci. B **15**, 412–428 (2014).
10.1631/jzus.B1400077
8. H. Zhou, Y. Xiong, Z. Liu, S. Hou, T. Zhou, *Cancer Cell. Int.* **21**, 402 (2021). 10.1186/s12935-021-02106-4
9. C. Zhang, L. Chang, Y. Yao, C. Chao, Z. Ge, C. Fan, H. Yu, B. Wang, J. Yang, *Front. Genet.* **12**, 771062 (2021). 10.3389/fgene.2021.771062
10. K. Hu, L. Yao, Z. Xu, Y. Yan, J. Li, *Front. Cell. Dev. Biol.* **10**, 832354 (2022). 10.3389/fcell.2022.832354
11. J. Liu, H. Shen, X. Chen, Y. Ding, H. Wang, N. Xu, L. Teng, *Genes (Basel)*. **13** (2022).
10.3390/genes13091582
12. A.A.T. Naqvi, S.A.M. Rizvi, M.I. Hassan, *Biochim. Biophys. Acta Mol. Basis Dis.* **1869**, 166561 (2023).
10.1016/j.bbadis.2022.166561
13. S. Lv, L. Ji, B. Chen, S. Liu, C. Lei, X. Liu, X. Qi, Y. Wang, E. Lai-Han Leung, H. Wang, L. Zhang, X. Yu, Z. Liu, Q. Wei, L. Lu, *Oncogene*. **37**, 1354–1368 (2018). 10.1038/s41388-017-0026-x
14. Y. Liao, K. Xu, *Asian J. Androl.* **21**, 279–290 (2019). 10.4103/aja.aja_53_18
15. R. Klukovich, E. Nilsson, I. Sadler-Riggelman, D. Beck, Y. Xie, W. Yan, M.K. Skinner, *Sci. Rep.* **9**, 2209 (2019). 10.1038/s41598-019-38741-1
16. F. Zhou, L. Chen, P. Lu, Y. Cao, C. Deng, G. Liu, *BMC Cancer*. **23**, 641 (2023). 10.1186/s12885-023-11108-6
17. X. Li, L. Li, X. Xiong, Q. Kuang, M. Peng, K. Zhu, P. Luo, *Diagnostics (Basel)*. **13** (2023).
10.3390/diagnostics13081393
18. D. Liao, X. Liu, L. He, Y. Yao, X. Yuan, P. Feng, C. Li, Y. Liu, *Iran. J Basic Med Sci.* **26**, 468–477 (2023).
10.22038/IJBMS.2023.64845.14281
19. L. Wang, L. Zhao, Y. Zhang, S. Shao, Q. Ning, X. Zhao, M. Luo, *Clin. Breast Cancer*. **23**, e206–e218 (2023). 10.1016/j.clbc.2023.02.007
20. A.M. Grimaldi, O. Affinito, M. Salvatore, M. Franzese, *Diagnostics (Basel)*. **12** (2022).
10.3390/diagnostics12102452
21. Z.Q. Zheng, G.Q. Yuan, N.L. Kang, Q.Q. Nie, G.G. Zhang, Z. Wang, *Front. Neurol.* **13**, 912039 (2022).
10.3389/fneur.2022.912039
22. X. Meng, R. Cao, X. Liu, B. Fu, L. Luo, M. Jiang, K. Wang, Y. Liu, Q. Zhu, C. Yang, L. Zhou, *Oncol. Lett.* **25**, 172 (2023). 10.3892/ol.2023.13758
23. J. Wang, B. Yang, X. Zhang, S. Liu, X. Pan, C. Ma, S. Ma, D. Yu, W. Wu, *Int. J. Oncol.* **62** (2023).
10.3892/ijo.2023.5484
24. L. Li, W. Zhang, J. Qiu, W. Zhang, M. Lu, J. Wang, Y. Jin, Q. Xi, *Stem Cells Int* 2023, 4500561 (2023)
10.1155/2023/4500561
25. Y. Xu, S. Pan, Y. Song, C. Pan, C. Chen, X. Zhu, *J. Cancer*. **11**, 5198–5209 (2020). 10.7150/jca.44475
26. Z. Yang, Q. Zi, K. Xu, C. Wang, Q. Chi, *Int. Immunopharmacol.* **90**, 107238 (2021).
10.1016/j.intimp.2020.107238

27. S. Zheng, P. Lv, J. Su, K. Miao, H. Xu, M. Li, Am. J. Transl Res. **11**, 1668–1682 (2019)
28. Y.J. Zhang, L.Y. Zhao, X. He, R.F. Yao, F. Lu, B.N. Lu, Z.R. Pang, Aging (Albany NY). **14**, 6227–6254 (2022). 10.18632/aging.204214
29. L.W. Brubaker, D.S. Backos, V.T. Nguyen, P. Reigan, T.M. Yamamoto, E.R. Woodruff, R. Iwanaga, M.F. Wempe, V. Kumar, C. Persenaire, Z.L. Watson, B.G. Bitler, Expert Opin. Ther. Targets. **27**, 361–371 (2023). 10.1080/14728222.2023.2218614
30. A. Di Costanzo, N. Del Gaudio, L. Conte, C. Dell'Aversana, M. Vermeulen, H. de The, A. Migliaccio, A. Nebbioso, L. Altucci, Oncogene. **37**, 2559–2572 (2018). 10.1038/s41388-018-0143-1

Figures

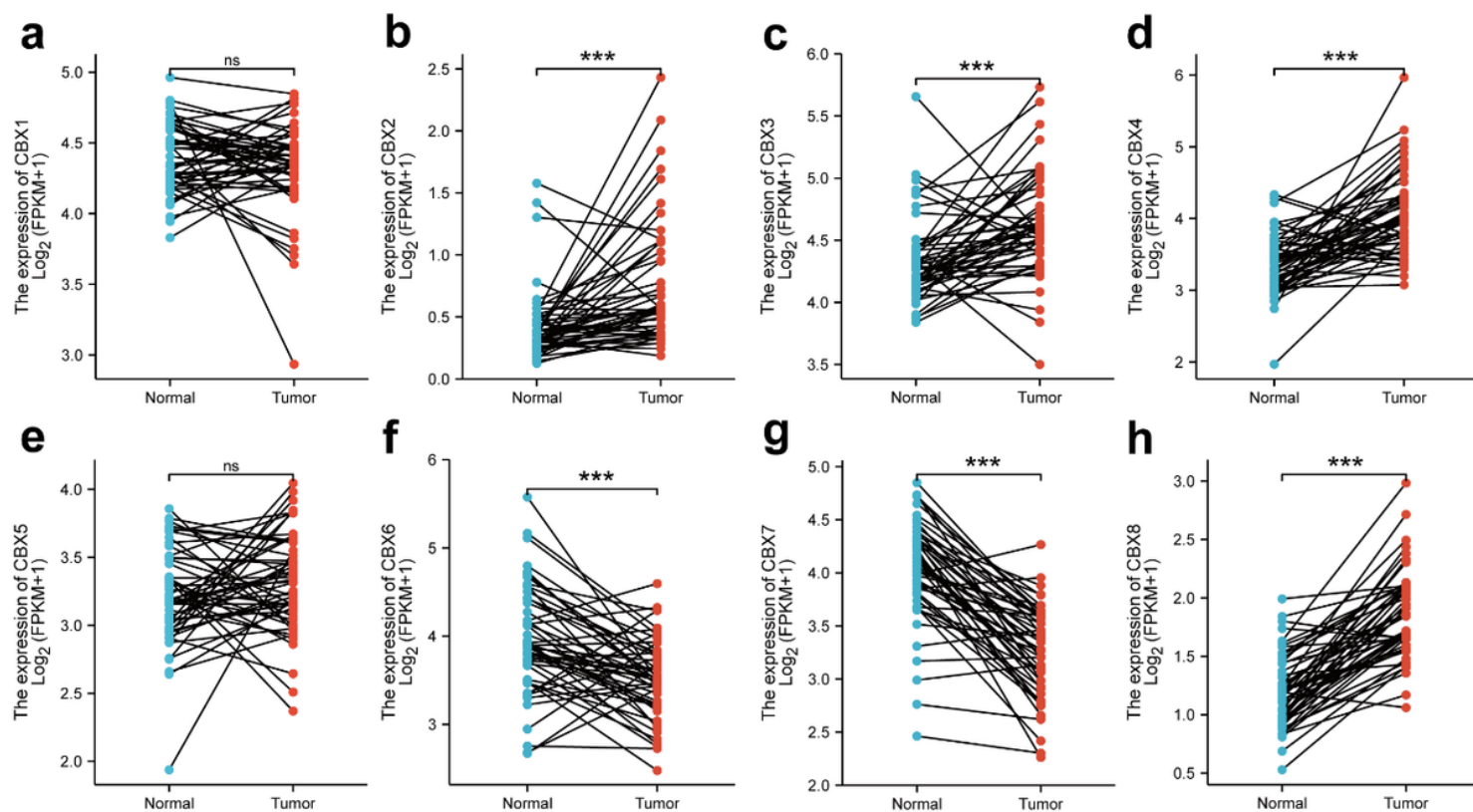


Figure 1

Expression of CBXs in PCa tumor tissues and adjacent non-tumor tissues. (a-h) Bar chart of CBX1(a), CBX2(b), CBX3(c), CBX4(d), CBX5(e), CBX6(f), CBX7(g) and CBX8(h) expression in PCa and adjacent non-tumor tissues. *** $P < 0.001$ by paired student's t -test, ns: non-significant

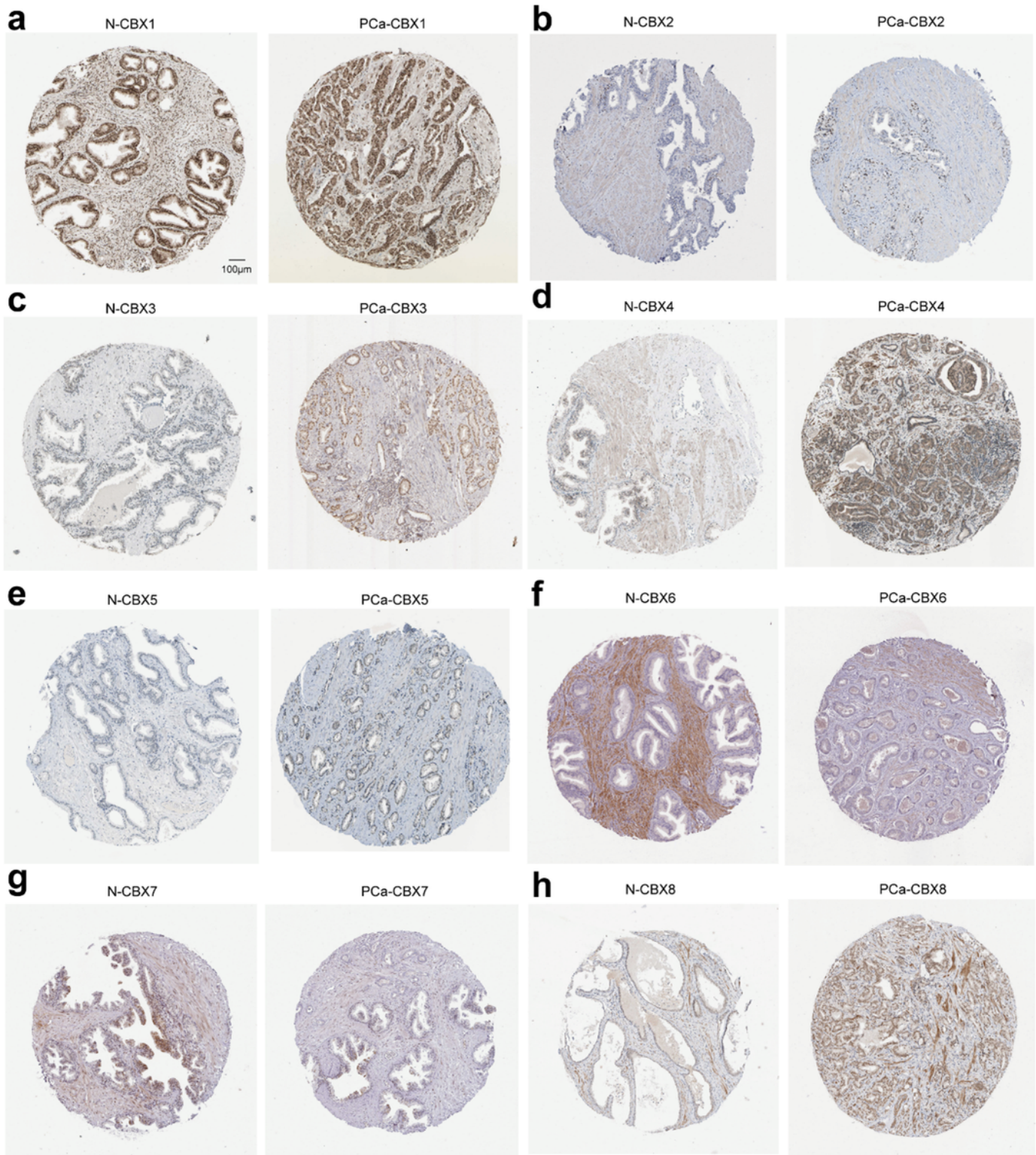


Figure 2

IHC of CBXs in adjacent non-tumor tissues and PCa tumor tissues. (a-h) Representative IHC images of CBX1(a), CBX2(b), CBX3(c), CBX4(d), CBX5(e), CBX6(f), CBX7(g) and CBX8(h) in adjacent non-tumor tissue and PCa tumor tissue

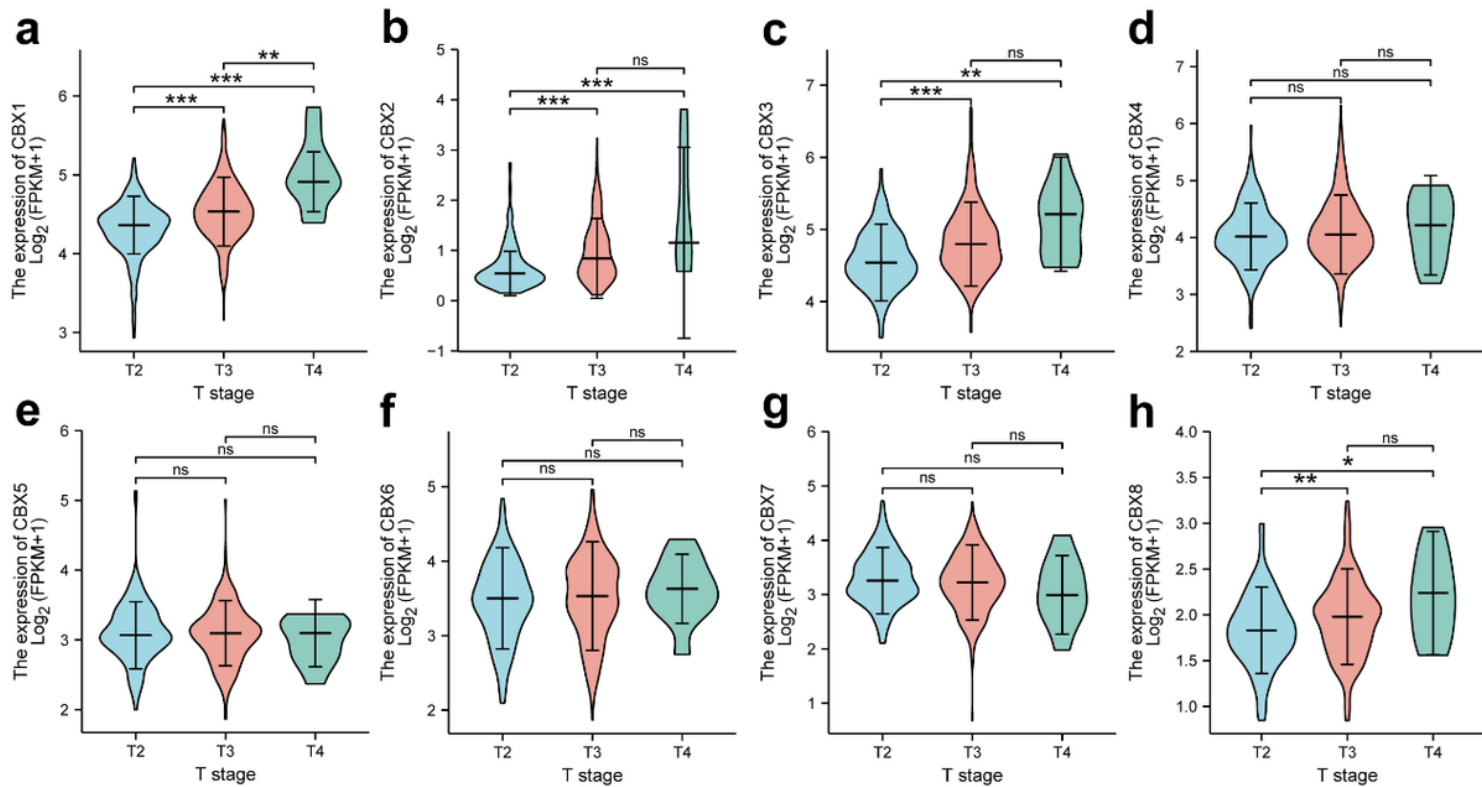


Figure 3

Violin plot of CBXs expression in PCa tissues of different T stages. (a-h) CBX1(a), CBX2(b), CBX3(c), CBX4(d), CBX5(e), CBX6(f), CBX7(g) and CBX8(h) expression in PCa tissues of different T stages. (* $P < 0.05$, ** $P < 0.01$, * $P < 0.001$)**

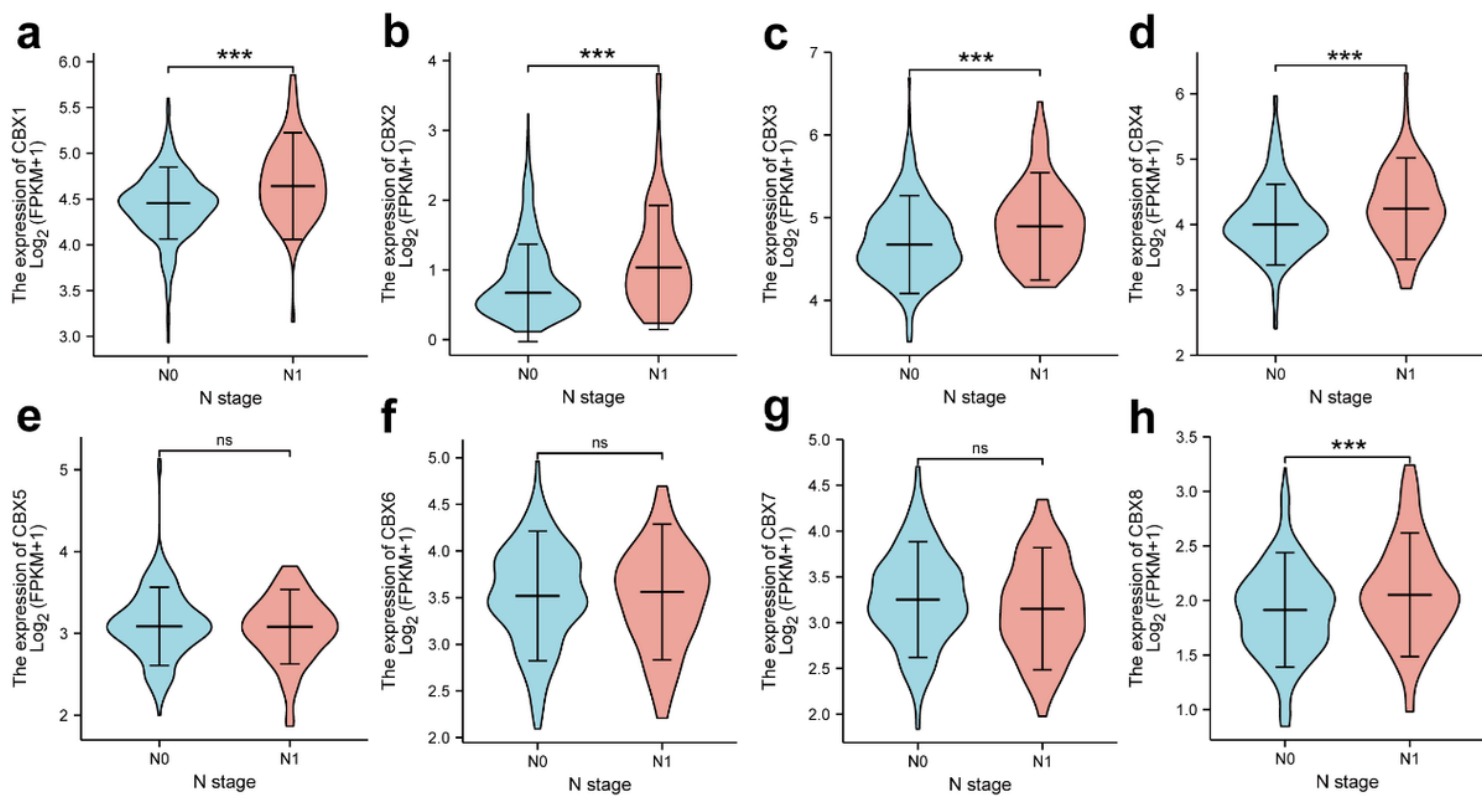


Figure 4

Violin plot of CBXs expression in PCa tissues of N0 and N1 stages. (a-h) CBX1(a), CBX2(b), CBX3(c), CBX4(d), CBX5(e), CBX6(f), CBX7(g) and CBX8(h) expression in PCa tissues of N0 and N1 stages. (*) $P < 0.001$)**

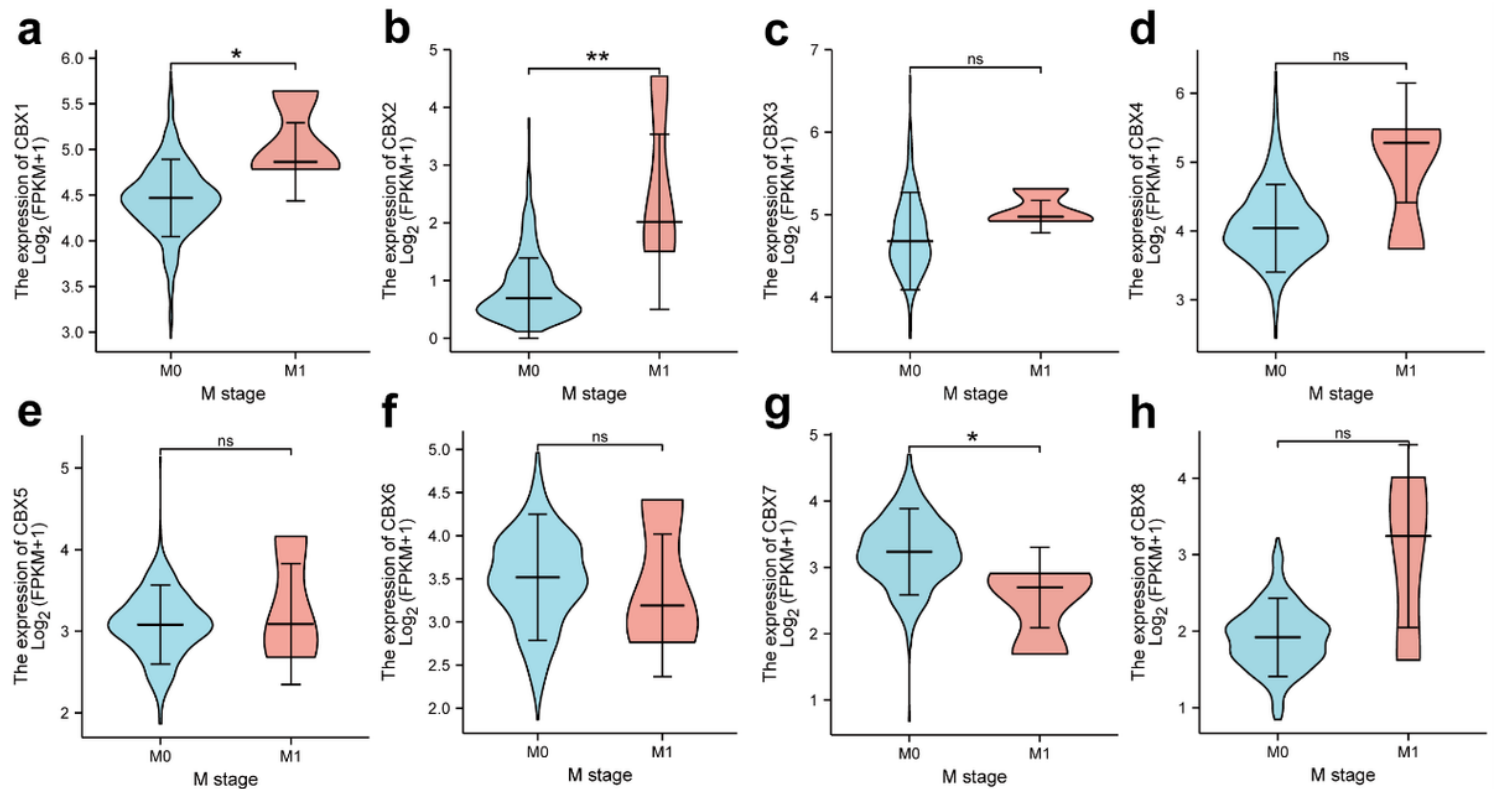


Figure 5

Violin plot of CBXs expression in PCa tissues of M0 and M1 stages. (a-h) CBX1(a), CBX2(b), CBX3(c), CBX4(d), CBX5(e), CBX6(f), CBX7(g) and CBX8(h) expression in PCa tissues of M0 and M1 stages. (* $P < 0.05$, ** $P < 0.01$)

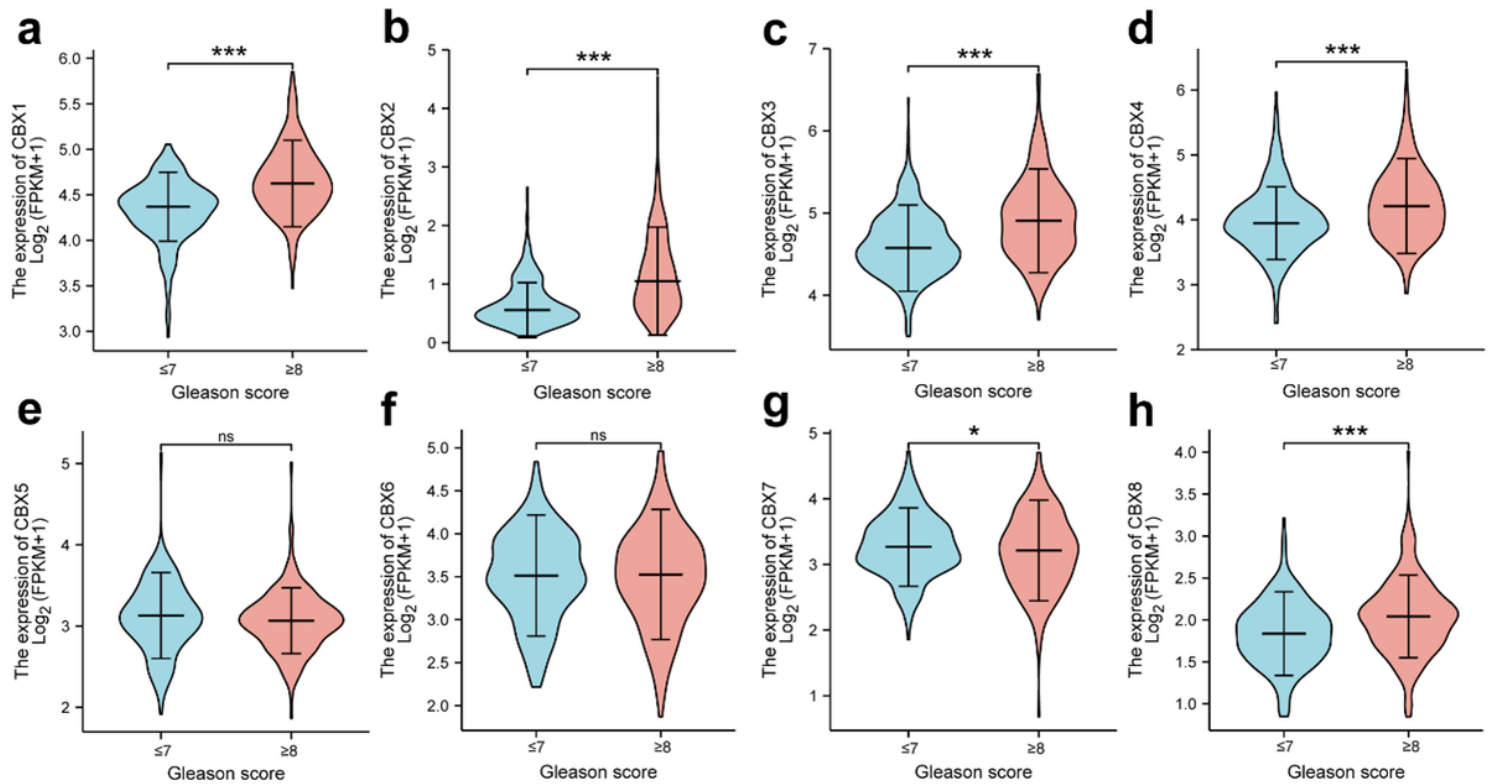


Figure 6

Violin plot of CBXs expression in PCa tissues of Gleason ≤ 7 and Gleason ≥ 8 groups. (a-h) CBX1(a), CBX2(b), CBX3(c), CBX4(d), CBX5(e), CBX6(f), CBX7(g) and CBX8(h) expression in PCa tissues of Gleason ≤ 7 and Gleason ≥ 8 groups (* $P < 0.05$, * $P < 0.001$)**

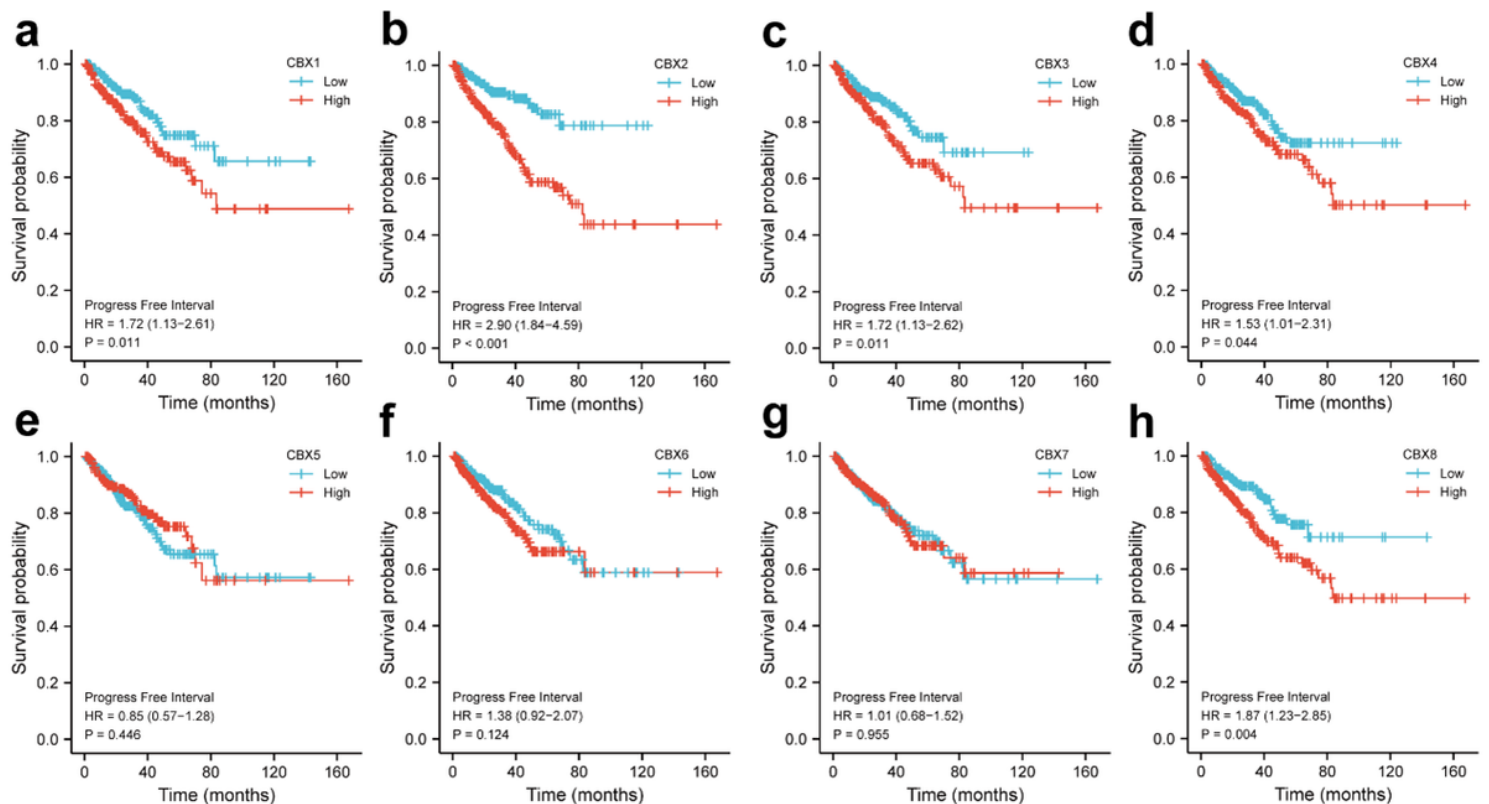


Figure 7

Survival curves of CBXs. (a-h) Relationships between mRNA expression levels of CBX1(a), CBX2(b), CBX3(c), CBX4(d), CBX5(e), CBX6(f), CBX7(g), CBX8(h) and the prognosis of patients with PCa

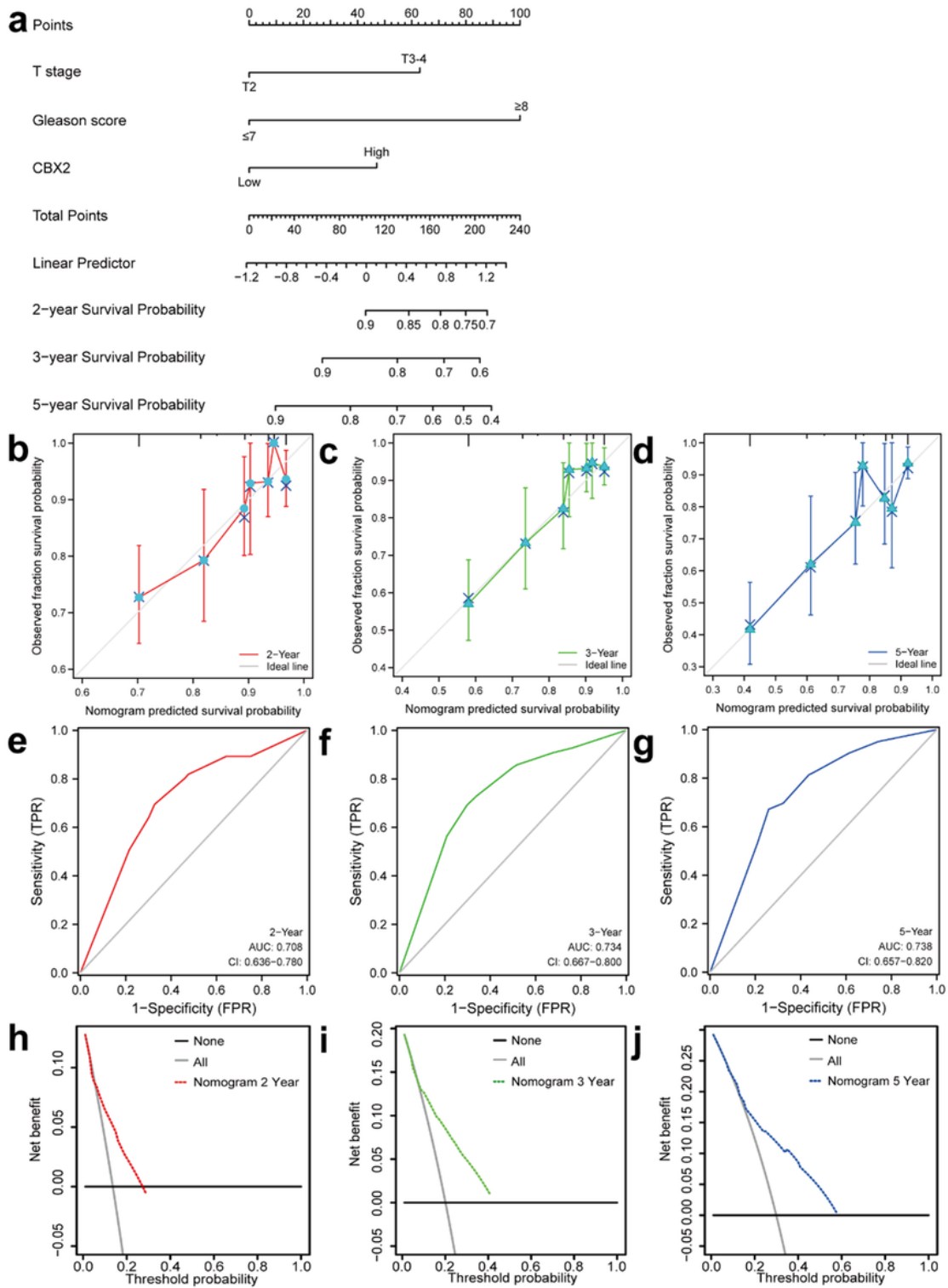


Figure 8

Construction of nomogram based on TCGA database. (a) Nomogram for predicting DFS of PCa patients based on CBXs expression levels and T, Gleason score. **(b-d)** Calibration curves for 2-year, 3-year and 5-year DFS of PCa. **(e-g)** ROC curves and AUC values for 2-year, 3-year and 5-year DFS of PCa. **(h-j)** DCA curves for 2-year, 3-year and 5-year DFS of PCa

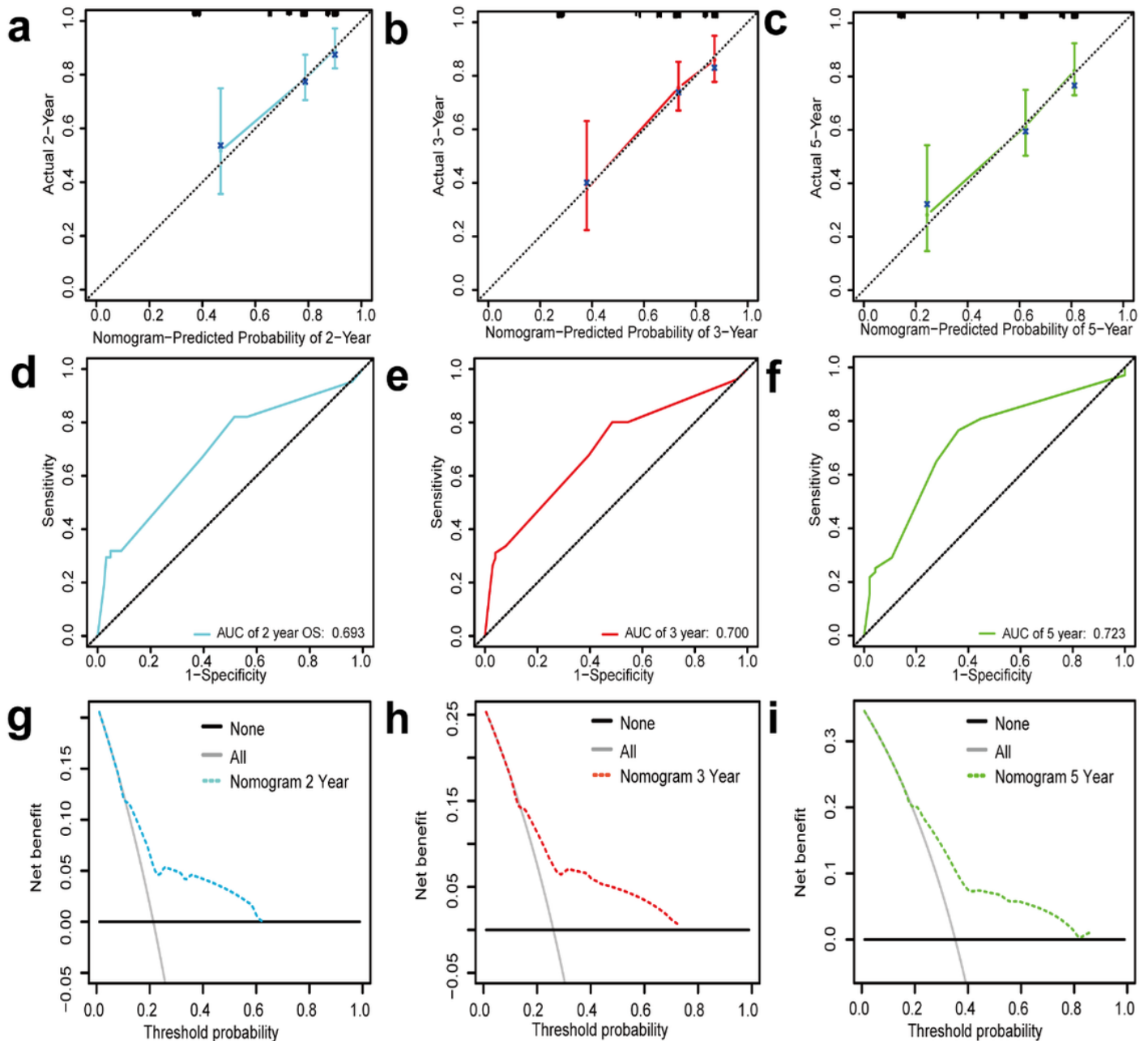


Figure 9

Validation of nomogram based on GEO database. (a-c) Calibration curves for 2-year, 3-year, and 5-year DFS of PCa. **(d-f)** ROC curves and AUC values for 2-year, 3-year and 5-year DFS of PCa. **(g-i)** DCA curves

for 2-year, 3-year and 5-year DFS of PCa

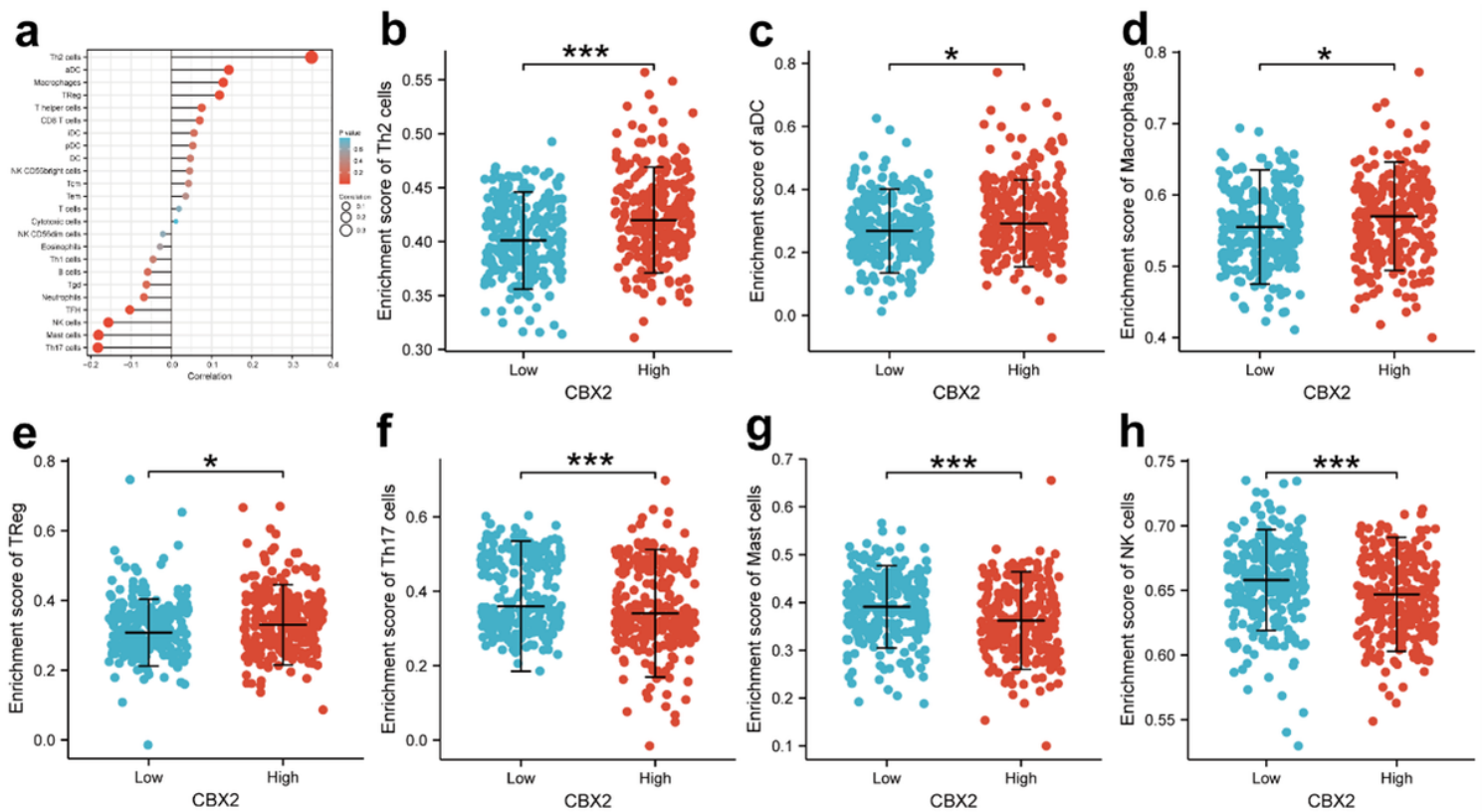


Figure 10

Results of ssGSEA algorithm analysis. (a) Lollipop plot showing the correlation between CBX2 and immune cell infiltration. **(b-h)** Infiltration levels of seven immune cells including Th2(b), aDC(c), macrophages(d), Treg(e), Th17(f), Mast cells(g) and NK cells(h) in PCa tissues of groups with CBX2 high and low expression (* $P < 0.05$, *** $P < 0.001$)

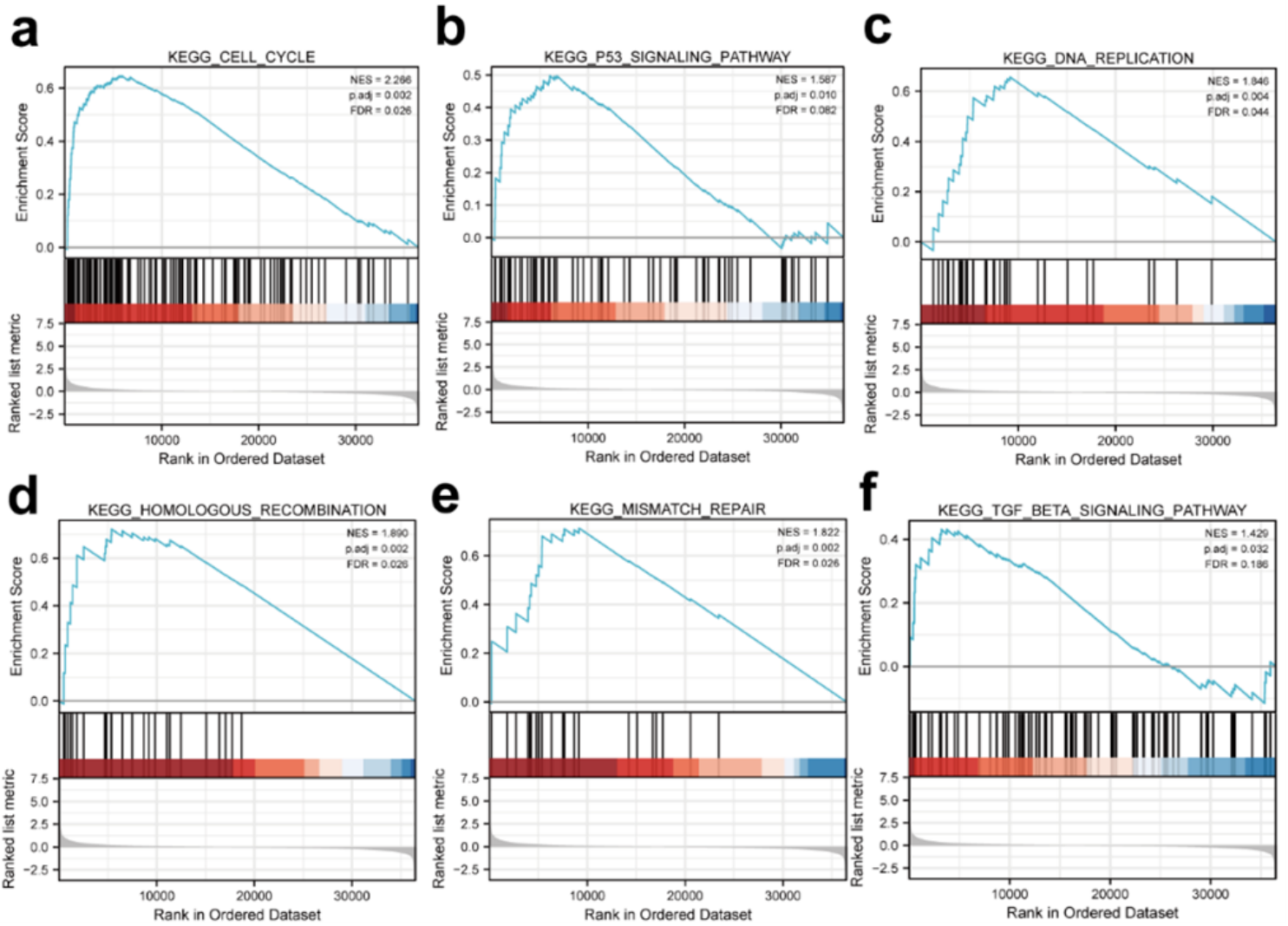


Figure 11

GSEA enrichment analysis of differentially expressed genes in groups with high and low expression of CBX2. (a-f) Pathways enriched in the group with high expression of CBX2

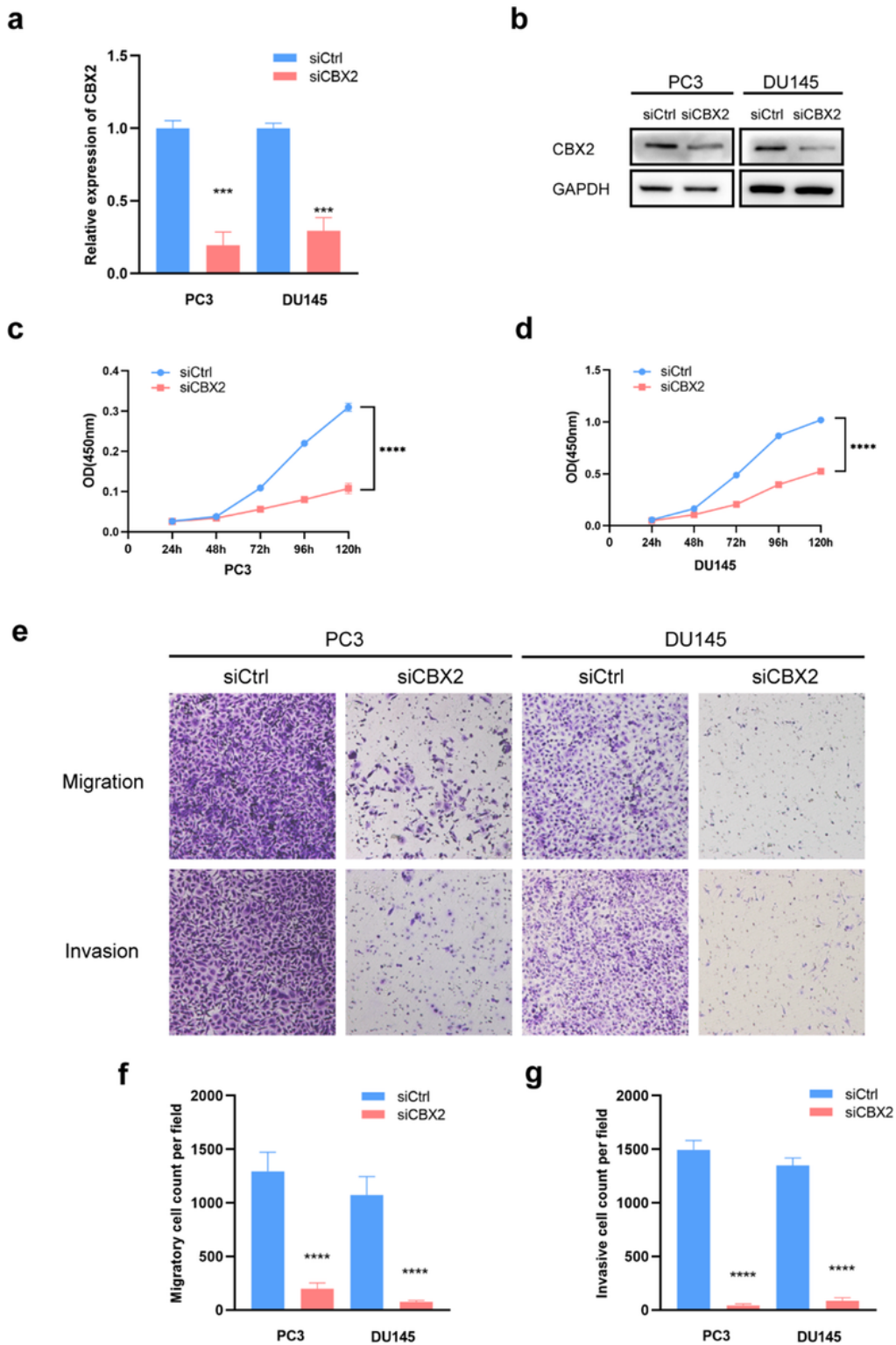


Figure 12

The effect of CBX2 on the proliferation, migration and invasion of PCa cells. [a-d] The mRNA (a) and protein (b) levels of CBX2 in PC3 and DU145 cells transfected with siCtrl and siCBX2. The effect of siCBX2 on the growth of PC3 (c) and DU145 (d) cells. (e-g) The effect of siCBX2 on the migration and invasion of PC3 and DU145 cells. *** $p < 0.001$, **** $p < 0.0001$, by unpaired student's t -test

Supplementary Files

This is a list of supplementary files associated with this preprint. Click to download.

- [Rcode.zip](#)
- [SupplementaryMaterials.pdf](#)